

TYPE I SUPERNOVAE. I. ANALYTIC SOLUTIONS FOR THE EARLY PART OF THE LIGHT CURVE

W. DAVID ARNETT

Enrico Fermi Institute, University of Chicago
 Received 1980 December 1; accepted 1981 August 6

ABSTRACT

Analytic solutions for light curves, effective temperatures, and broad-band colors of Type I supernovae are presented. The method is generalized to include effects of finite (large) initial radius and increasing transparency to γ -rays and to thermal photons. A theoretical construct, the "blackbody supernova," is introduced. Many observed features of Type I supernovae are shown to be reproduced by the theory. For a given composition it is shown that the homogeneity of spectral evolution is a necessary consequence of the thermonuclear model but only a possible consequence of the gravitational collapse model. Comparison with 1970j and 1972e suggests a variation in explosion energy of a factor of 2, and a corresponding variation in intrinsic luminosity at maximum light; such variation can be identified in a distance-independent way.

Subject headings: nucleosynthesis — stars: supernovae

I. INTRODUCTION

In a previous paper (Arnett 1980), analytic solutions for the light curves of Type II supernovae were presented, compared to detailed numerical solutions, and used to analyze some observational results. In this paper the method is generalized to include Type I supernovae by including the effects of the radioactive decay of ^{56}Ni and ^{56}Co . The solutions obtained are "analytic" in the sense that they are expressed in terms of tabulated functions or integrals that are easy to do numerically (reduction to quadrature).

In § II the method of solution is illustrated in detail for the simplest case: small initial radii and the energy source simply ^{56}Ni decay. The physical assumptions are presented and the mathematical behavior is analyzed.

In § III the method is generalized to include the effects of large radii ($R \gg 10^{13}$ cm). It is shown that the solutions are essentially a combination of those for Type II supernovae (Arnett 1980) and those found in § II. Implications of these solutions for observations and for presupernova structure are discussed.

In § IV the method is generalized further to include ^{56}Co decay and increasing transparency to γ -rays and to thermal photons. A theoretical construct, the "blackbody supernova," is introduced so that a (crude) comparison with observed supernovae can be made.

In § V the results are discussed in relation to other recent work and several prospects for improvements and extensions are presented.

II. THE METHOD

a) Physical Assumptions

In order to reduce the problem to a tractable form, some simplification must be made. The value of the solutions lies in the fact that these assumptions really are physically plausible; see Colgate and McKee (1969) and Arnett (1979). The assumptions are:

1. *Homologous expansion.* This is a natural consequence of a spherical shock (see Arnett 1980, to be denoted A80).

2. *Radiation pressure dominant.* For the energies and densities encountered this approximation is superb. The equation of state is therefore $E = aT^4V$ and $P = E/3V$.

3. *^{56}Ni present in ejected matter.* This feature is crucial for Type I behavior.

4. *^{56}Ni distribution somewhat peaked toward the center of the ejected mass.* This mathematically convenient assumption (see below) is actually a good approximation for a variety of plausible models.

A fifth simplification, which is not necessary but may be a physically relevant one, is that the initial radius be small [$R(0) \ll 10^{14}$ cm]. This restriction will be removed in § III.

As before (A80), a constant (effective) opacity will be assumed; Thomson scattering may dominate the transport cross section, but the absorption cross section will be modified from the static case (Karp *et al.* 1977).

To simplify the exposition of the method, it will be further assumed for this section that the energy source is only the exponential release of nuclear energy by ^{56}Ni decay (see eq. [9] below). This restriction will be removed in the following sections.

Finally, spherical symmetry is assumed.

b) Derivation of Solutions

The thermal state of the expanding matter evolves in time according to the first law of thermodynamics,

$$\dot{E} + P\dot{V} = -\partial L/\partial m + \varepsilon, \quad (1)$$

where

$$L/4\pi r^2 = -(\lambda c/3)\partial aT^4/\partial r \quad (2)$$

and ε is the energy release, per unit mass, from radioactive decay. Note that the mean free path is $\lambda = 1/\rho\kappa$ and $V = 1/\rho$ is the specific volume.

For homologous expansion in a coasting phase,

$$R(t) = R(0) + v_{sc}t \quad (3)$$

and

$$v(x) = xv_{sc}, \quad (4)$$

where

$$x = r(m, t)/R(t) \quad (5)$$

is a dimensionless radius and v_{sc} is the velocity scale. Therefore,

$$\dot{V}/V = 3\dot{R}/R = 3v_{sc}/R. \quad (6)$$

Now, let

$$V(r, t) = V(0, 0)[R(t)/R(0)]^3/\eta(x), \quad (7)$$

where $\eta(x)$ is the dimensionless run of density and is time independent for our assumptions.

As in A80, let

$$T(r, t)^4 = \psi(x)\phi(t)T(0, 0)^4R(0)^4/R(t)^4. \quad (8)$$

Further, let

$$\varepsilon = \varepsilon_{\text{Ni}}^0 \xi(x) e^{-t/\tau_{\text{Ni}}}, \quad (9)$$

where $\varepsilon_{\text{Ni}}^0 = 4.78 \times 10^{10}$ ergs $\text{g}^{-1} \text{s}^{-1}$, $\tau_{\text{Ni}} = 7.605 \times 10^5$ s, and $\xi(x)$ gives the distribution of ^{56}Ni . Denote

$$\tau_0 \equiv 3R(0)^2 \kappa(0)/V(0, 0) \alpha c \quad (10)$$

and

$$\alpha \equiv -\frac{1}{x^2 \psi(x)} \frac{\partial}{\partial x} \left(\frac{x^2}{\eta(x)} \frac{\partial \psi}{\partial x} \right). \quad (11)$$

This follows A80 with κ taken to be constant; see equations (8)–(10) in that paper. Using these expressions, (1) reduces to

$$\alpha/\tau_0 = R(0)(\partial\phi/\partial t)/R(t)$$

$$-\left[\frac{\varepsilon_{\text{Ni}}^0}{aT(0, 0)^4 V(0, 0)} \right] \left[\frac{\xi(x)\eta(x)}{\psi(x)} \right] e^{-t/\tau_{\text{Ni}}}. \quad (12)$$

Now if we assume that

$$b \equiv \xi(x)\eta(x)/\psi(x) \quad (13)$$

is constant for any x , then from (11) α depends only on x while in (12) it depends only on t . The equations are then separable, as α must be a constant. Thus (13) is the quantitative expression of approximation (4) in § IIa above. It says that the volume emission of radioactive decay energy, $\xi(x)\eta(x)$, is proportional to the radiation energy per unit volume, $\psi(x)$. This is not strictly true. However, it turns out to be a surprisingly good approximation. This is partially due to the concentration of ^{56}Ni energy deposition toward the inner matter in many models, which is qualitatively similar to the radiation energy distribution. It is also due to the relative insensitivity of many features of the solutions to the precise constancy of b in (13).

Solutions of (11), and the corresponding spatial boundary conditions, were discussed at length in A80; those results will be used here without further comment.

The time dependence is governed by (12) which becomes

$$\dot{\phi} + \phi R(t)/R(0)\tau_0 = \tilde{\varepsilon} R(t) e^{-t/\tau_{\text{Ni}}}/R(0), \quad (14)$$

where

$$\tilde{\varepsilon} = b\varepsilon_{\text{Ni}}^0/aT(0, 0)^4 V(0, 0). \quad (15)$$

Let

$$\dot{u} = R(t)/R(0)\tau_0; \quad (16)$$

so, using (3),

$$u(t) = t/\tau_0 + (t/\tau_m)^2, \quad (17)$$

where

$$\tau_m^2 \equiv 2R(0)\tau_0/v_{sc} = 2\tau_0\tau_h, \quad (18)$$

and

$$\tau_h = R(0)/v_{sc}. \quad (19)$$

The time scale τ_m determined the behavior of the Type II light curve, and will be a fundamental parameter here as well. It is essentially the geometric mean of the expansion and the diffusion time scales.

Now,

$$R(t)\tilde{\epsilon}e^{-t/\tau_{Ni}}/R(0) = \dot{\phi} + \phi\dot{u} = e^{-u}\frac{d}{dt}(\phi e^u). \quad (20)$$

For simplicity we will consider the case of $R(0)$ small; the more general case is given later. Before we take the limit $R(0) \rightarrow 0$, we need to consider the diffusion time τ_0 more carefully. Denote

$$I_M \equiv \int_0^1 \eta(x)x^2 dx = V(0,0)M/4\pi R(0)^3, \quad (21)$$

where M is the total mass ejected, and use this to rewrite (10) as

$$\tau_0 = \kappa M/\beta c R(0) \quad (22)$$

where

$$\beta \equiv 4\pi(\alpha I_M/3). \quad (23)$$

From Table 2 of A80 we see that $\beta \approx 13.7$ for a variety of density distributions. Now, $\tau_0 R(0)$ is constant for any $R(0)$, so as $R(0)$ goes to zero,

$$u(t) \sim (t/\tau_m)^2. \quad (24)$$

To evaluate $\tilde{\epsilon}$, we need to use some identities. The mass of ^{56}Ni initially present must be

$$M_{Ni}^0 = 4\pi R(0)^3 V(0,0)^{-1} \int_0^1 \xi(x)\eta(x)x^2 dx. \quad (25)$$

The total thermal energy content E_{Th} is obtained by integrating aT^4 over the volume, using (8); this gives

$$E_{Th}(t) = 4\pi R(0)^3 aT(0,0)^4 I_{Th}\phi(t)R(0)/R(t), \quad (26)$$

where

$$I_{Th} \equiv \int_0^1 \psi(x)x^2 dx. \quad (27)$$

Now (21), (25), and (13) give

$$b = \left(\frac{M_{Ni}^0}{M}\right) \frac{I_M}{I_{Th}}. \quad (28)$$

Using (21) and (26) to eliminate $T(0,0)$ and $V(0,0)$ from (15) gives

$$\tilde{\epsilon} = \epsilon_{Ni}^0 M_{Ni}^0 \phi(0)/E_{Th}(0), \quad (29)$$

which is finite as $R(0) \rightarrow 0$ if $E_{Th}(0) > 0$ (as we will assume). Using (24) and (29), we find

$$\phi(t) = \frac{\epsilon_{Ni} M_{Ni}^0 \tau_0}{E_{Th}(0)} \Lambda(x, y) + \exp(-x^2), \quad (30)$$

where

$$\Lambda(x, y) = \exp(-x^2) \int_0^x \exp(-2zy + z^2) 2z dz, \quad (31)$$

$$x = t/\tau_m, \quad (32)$$

and

$$y = \tau_m/2\tau_{Ni}. \quad (33)$$

Here $\phi(0)$ is an extra scale factor and has been set to 1. Considerable expansion has occurred since the explosion because we assume $R(0) \ll 10^{14}$ cm, so $\epsilon_{Ni} M_{Ni}^0 \tau_0 \gg E_{Th}(0)$ and the Λ term dominates the e^{-x^2} term in (30).

To obtain the luminosity at the surface, we substitute (8) into (2) to find

$$L(1, t) = \frac{16\pi^2 acT(0,0)^4 R(0)^4 I_M \phi(t)}{3\kappa M} \left(-\frac{x^2}{\eta} \frac{\partial \psi}{\partial x}\right)_{x=1}. \quad (34)$$

Integrating (11) by parts and evaluating at $x=0, 1$ gives

$$\left(-\frac{x^2}{\eta} \frac{\partial \psi}{\partial x}\right)_{x=1} = \alpha I_{Th}. \quad (35)$$

Using (22), (23), and (26),

$$L(1, t) = E_{Th}(0)\phi(t)/\tau_0 = \epsilon_{Ni} M_{Ni}^0 \Lambda(x, y). \quad (36)$$

The decay of ^{56}Ni produces ^{56}Co which also decays. Even if all the ^{56}Co γ -rays escape, the positron kinetic energy will heat the matter and thus provide additional luminosity (see Arnett 1979; Colgate and McKee 1969). Thus until the positrons also escape, the "tail" will have a bolometric luminosity *at least as large as*

$$\Lambda_{Co}(t) = M_{Ni}^0 \epsilon_{Co}^+ e^{-t/\tau_{Co}}, \quad (37)$$

where $\epsilon_{Co}^+ = 2.561 \times 10^8$ ergs $\text{g}^{-1} \text{s}^{-1}$ and $\tau_{Co} = 9.822 \times 10^6$ s. This corresponds to

$$\Lambda_{Co}(xy) = 5.36 \times 10^{-3} \exp(-0.1548 xy). \quad (38)$$

A careful estimate of the effective temperature would involve the effects of a transparency wave moving into the expanding matter. If this effect is ignored, a simple expression for the effective temperature results; it is valid if T_e is above the recombination temperature. A similar approximation was used for Type II supernovae (see Figs. 2 and 3 of Arnett 1980), and worked surprisingly well when compared to numerical calculations which included the transparency wave. Using

$$L(1, t) = 4\pi R(t)^2 \sigma T_e(t)^4, \quad (39)$$

and $R(t) \approx v_{sc} t$ with (36) gives

$$T_e(t)^4 = (\epsilon_{Ni} M_{Ni}^0 / 16\pi\sigma v_{sc}^2 \tau_{Ni}^2) \Lambda(x, y) / (xy)^2 \quad (40)$$

or

$$T_e(t) = 15,493 \text{ K} \left(\frac{M_{Ni}^0}{M_{\odot}} \right)^{1/4} \times \left(\frac{10^9 \text{ cm s}^{-1}}{v_{sc}} \right)^{1/2} \left[\frac{\Lambda(x, y) k}{x^2 y^2} \right]^{1/4}. \quad (41)$$

Note that for given x and y , the effective temperature scale depends only on the mass of ^{56}Ni and the scaling velocity. A more detailed discussion of the effective temperature will be given in § IV.

c) *Mathematical Behavior*

The function $\Lambda(x, y)$ is a one-parameter (y) family of curves. The parameter

$$y = \tau_m / 2\tau_{Ni} = (2\kappa M / \beta c v_{sc})^{1/2} / 2\tau_{Ni} \quad (42)$$

is small for small $\kappa M / v_{sc}$. In the limit $y \ll x$,

$$\Lambda(x, y) \approx e^{-2yx} - \exp(-x^2) \approx e^{-t/\tau_{Ni}} - \exp\left[-(t/2y\tau_{Ni})^2\right]. \quad (43)$$

For short "effective diffusion time" τ_m , the luminosity follows the radioactive decay (after a rapid rise).

For $y \gg x$, (31) becomes

$$\Lambda(x, y) \approx [1 - e^{-2xy}(1 + 2xy)] / 2. \quad (44)$$

Note that $2xy = t/\tau_{Ni}$. This is a sort of saturation curve which rises to a maximum luminosity in a few decay times τ_{Ni} . The solution may also be derived directly from (1) if the loss of energy due to radiative diffusion is assumed inconsequential. Such an approximation is appropriate to the rising part of the light curve, when the

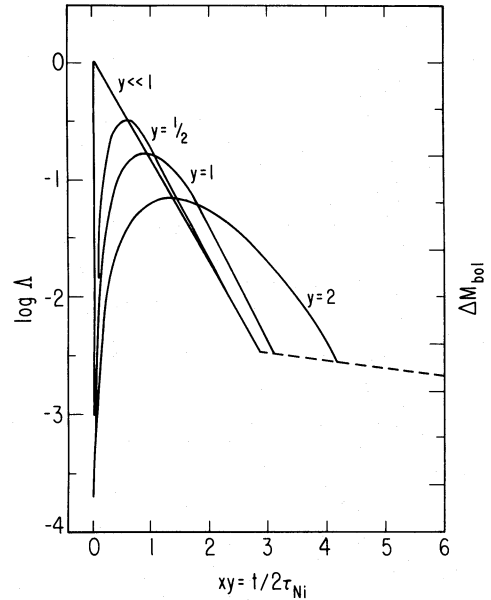


FIG. 1.—Bolometric magnitude versus time for the decay of ^{56}Ni above and for small initial radii. The curves are labeled with the crucial parameter y . The base 10 logarithm of Λ is plotted as a function of time (xy) in units of 17.6 days. The dashed line is the corresponding curve for positron kinetic energy release from ^{56}Co decay.

diffusion times are long. For small xy , (44) gives

$$\Lambda(x, y) \approx x^2 \quad (45)$$

for all y .

Figure 1 shows the behavior of $\Lambda(x, y)$ for $y = 0, 0.5, 1$, and 2. Here "y = 0" means only $y \ll x$. The curves are plotted as a function of $xy = t/2\tau_{Ni}$, so that an interval $\Delta xy = 1$ corresponds to 17.6 days. Larger values of y mean longer effective diffusion times; thus the width in time of the peak increases. The dashed line corresponds to the energy released by ^{56}Co decay only in the form of positron kinetic energy; that is, $\Lambda_{Co}(xy)$ from (38).

By direct differentiation of (31), we find that the maximum in the light curve function Λ , for given y , occurs at

$$\Lambda(x, y) = e^{-2xy}. \quad (46)$$

At maximum light the diffusion loss equals the radioactive input, a result obtained previously (Arnett 1979). Because $2xy = t/\tau_{Ni}$, this means that the simple Ni decay curve ("instant diffusion") intersects each luminosity curve at its maximum value (for given y). This behavior may be seen in Figure 1. Note that the $y \ll 1$ curve is essentially $\exp(-2xy)$; see (43). From (46) we see that curves which have their maximum at later times (larger xy), and therefore broader luminosity peaks, will

TABLE I
THE LIGHT CURVE FUNCTION $\Lambda(x, y)$

xy	$\Lambda(x, 0.5)$	$\Lambda(x, 0.65)$	$\Lambda(x, 0.8)$	$\Lambda(x, 1)$	$\Lambda(x, 1.2)$	$\Lambda(x, 1.5)$	$\Lambda(x, 2)$
0.....	0	0	0	0	0	0	0
0.2 ...	1.13 (-1)	6.93 (-2)	4.65 (-2)	3.0 (-2)	2.11 (-2)	1.36 (-2)	7.65 (-3)
0.4 ...	2.73 (-1)	1.85 (-1)	1.30 (-1)	8.76 (-2)	6.25 (-2)	4.09 (-2)	2.34 (-2)
0.6 ...	3.19 (-1)	2.51 (-1)	1.92 (-1)	1.38 (-1)	1.02 (-1)	6.83 (-2)	4.00 (-2)
0.8 ...	2.64 (-1)	2.46 (-1)	2.10 (-1)	1.63 (-1)	1.27 (-1)	8.90 (-2)	5.39 (-2)
1.0 ...	1.83 (-1)	1.97 (-1)	1.89 (-1)	1.63 (-1)	1.35 (-1)	1.00 (-1)	6.34 (-2)
1.2 ...	1.18 (-1)	1.39 (-1)	1.49 (-1)	1.44 (-1)	1.28 (-1)	1.02 (-1)	6.83 (-2)
1.4 ...	7.57 (-2)	9.11 (-2)	1.06 (-1)	1.15 (-1)	1.12 (-1)	9.61 (-2)	6.90 (-2)
1.6 ...	4.90 (-2)	5.81 (-2)	7.11 (-2)	8.54 (-2)	9.04 (-2)	8.52 (-2)	6.63 (-2)
1.8 ...	3.20 (-2)	3.70 (-2)	4.57 (-2)	5.94 (-2)	6.88 (-2)	7.16 (-2)	6.12 (-2)
2.0 ...	2.10 (-2)	2.38 (-2)	2.89 (-2)	3.94 (-2)	4.96 (-2)	5.75 (-2)	5.44 (-2)
2.4 ...	9.22 (-3)	1.01 (-2)	1.17 (-2)	1.60 (-2)	2.27 (-2)	3.27 (-2)	3.94 (-2)
2.8 ...	4.07 (-3)	4.38 (-3)	4.89 (-3)	6.29 (-3)	9.26 (-3)	1.62 (-2)	2.56 (-2)
3.2 ...	1.81 (-3)	1.92 (-3)	2.10 (-3)	2.54 (-3)	3.58 (-3)	7.10 (-3)	1.51 (-2)
3.6 ...	8.03 (-4)	8.48 (-4)	9.14 (-4)	1.06 (-3)	1.39 (-3)	2.85 (-3)	8.21 (-3)
4.0 ...	3.58 (-4)	3.76 (-4)	4.01 (-4)	4.55 (-4)	5.61 (-4)	1.09 (-3)	4.10 (-3)

necessarily have lower luminosity at maximum (other things being equal). This qualitative behavior reminds one of the observed behavior of the "fast" and "slow" supernovae of Barbon, Ciatti, and Rosino (1973); see § IVc.

Table I gives the light curve function $\Lambda(x, y)$; values are presented for $y=0.5, 0.65, 0.8, 1, 1.2, 1.5,$ and 2 , from $xy=0$ to the xy at which Λ falls below Λ_{Co} . This covers the range that is suggested by the observational data. Although $\Lambda(x, y)$ can be reduced to elementary functions plus an error function, that expression is awkward to evaluate; the table is far more convenient to use.

III. SOLUTIONS FOR LARGE INITIAL RADIUS

a) Mathematical Development

In the discussion following (20) above, the initial radius $R(0)$ was assumed to be small. Let us relax that restriction. Direct integration of (20) gives

$$\phi(t) = \phi(0) \left[e^{-u(x)} + (\epsilon_{Ni} M_{Ni} \tau_0 / E_{Th(0)}) \Omega(x, y, w) \right], \quad (47)$$

where

$$u(x) = wx + x^2, \quad w = (2\tau_h / \tau_0)^{1/2},$$

and

$$\Omega(x, y, w) = e^{-u(x)} \int_0^x (w + 2z) e^{-2yz + uz} dz. \quad (48)$$

Again we may choose $\phi(0)=1$ with no loss of generality. If we let $w \rightarrow 0$, then $\Omega(x, y, w) \rightarrow \Omega(x, y, 0) = \Lambda(x, y)$,

and our previous solution is recovered. Recall that the luminosity is proportional to $\phi(t)$; see (36).

However, if we set $\epsilon_{Ni} M_{Ni}^0$ to zero, then we find $\phi(t) = e^{-u(x)}$ which is the result previously obtained for Type II supernovae; see equation (14) of A80. This luminosity is due to diffusion in the expanding mass after instantaneous (shock) heating at $t=0$, and corresponds to the Lasher (1975) model of Type I supernovae.

This part of the solution in particular may need to be corrected for transient effects (see § VIII in A80). Schurmann (1982) has examined similar simple radioactive models of Type I supernovae by numerical methods. One of his results was the independent discovery of this "two-solution" behavior.

b) Observational Consequences

The behavior of the instantaneous (shock) part of (47), $e^{-u(x)}$, has an important qualitative difference from that of the radioactive part which is proportional to Ω . Because $e^{-u(x)}$ is large at early times when the radius is smallest, the effective temperature must be much higher at these early times. Although the contribution of $e^{-u(x)}$ to the bolometric luminosity declines with time, the observed luminosity may rise due to bolometric corrections if the light shifts from ultraviolet into visible wavelengths.

In Figure 2a are displayed the bolometric luminosities [as $\Lambda(x, y)$] as a function of time, for initial radius having values $R(0)/10^{14}$ cm = 0, 0.1, 0.3, and 1. Other parameters of these models are $M = 1.45 M_{\odot}$, $M_{Ni} = 0.7 M_{\odot}$, $v_{sc} = 1.2 \times 10^9$ cm s⁻¹, and $\kappa = 0.08$ g cm⁻². For completeness the radioactive energy source included ⁵⁶Co effects as described in the following section; this had no effect on the qualitative behavior discussed here. Two days after explosion ($xy \approx 0.1$) the bolometric

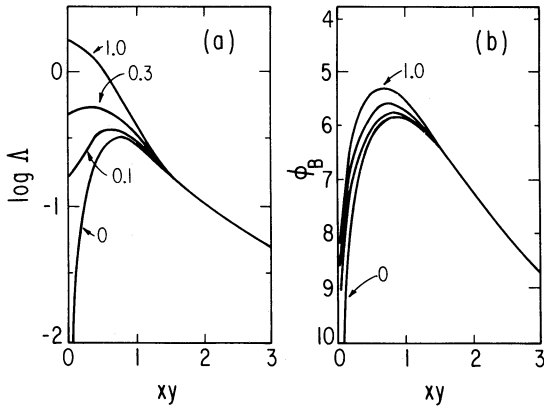


FIG. 2.—The effects of large initial radii. (a) The logarithm of bolometric luminosity Δ versus time ($xy = t/2\tau_{\text{Ni}}$) for initial radii $R(0) = (0, 0.1, 0.3, \text{ and } 1) \times 10^{14}$ cm. The large luminosity at early time is due to cooling of an extended envelope which has been shock-heated. (b) The B magnitude (actually ϕ_B as defined in § IV) versus time for the same initial radii as in Fig. 2a. Most of the extra luminosity emerges not in the *UBV* bands, but rather in the far-ultraviolet.

luminosity of the $R(0) = 10^{14}$ cm model is about 100 times larger than that of the $R(0) \approx 0$ model, and the effective temperature of the larger model is about 50,000 K.

This analysis is cautious in the sense that it ignores two effects which could further *increase* the early luminosity. There is presently some disagreement as to the strength of the burst of radiation due to the eruption of the supernova shock into the presupernova photosphere (Epstein 1980; Chevalier and Klein 1979; Falk 1978; Lasher and Chan 1979). Such a burst should be added to the luminosity calculated here. The second effect arises from the requirement that the initial temperature distribution be the lowest order eigenfunction of (11). A shock is expected to heat the outer layers more than this; this gives a larger luminosity at early times (see A80, § VIII).

These uncertainties regarding the very early behavior, while interesting in their own right, do not affect our interpretation of the usual phenomena observed as a Type I supernova. Note the dramatic convergence of the bolometric luminosity shown in Figure 2a at $xy \approx 1$ (17.6 days after explosion). The size of the initial radius affects primarily the premaximum part of the light curve. For those wavelengths usually observed, bolometric corrections will further reduce the differences between large and small initial radii. The formation of the spectrum in Type I supernovae is not well understood. If we make the crude approximation that the radiation is like that of a blackbody, then some qualitative understanding of the bolometric corrections can be gained. Figure 2b gives the corresponding B magnitudes for such a “blackbody supernova”; see the next section for details. The shapes

of the curves are now similar. Let us compare the extreme cases, $R(0) = 0$ and 10^{14} cm. The peak is shifted ($\Delta xy \approx -0.2$ or 3.5 days earlier) and the B luminosity is brighter by 0.5 mag for the larger radius. One might expect the U band to show greater differences, but in fact the changes are similar to those in the B band. The brightness change is slightly larger ($\Delta U \approx -0.7$).

If the envelope of the presupernova were in hydrostatic equilibrium, then the size of the initial radius would be constrained. Suppose the core of the presupernova has a mass $M_{\text{core}} \lesssim 1.4 M_{\odot}$ and a luminosity at the edge of the core is less than the Eddington limit, $4\pi cGM_{\text{core}}/\kappa$. The radius is then

$$R \lesssim 2 \times 10^{13} \text{ cm} \left(\frac{0.2 \text{ cm}^2 \text{ g}^{-1}}{\kappa} \right)^{1/2} \left(\frac{6000 \text{ K}}{T_e} \right)^2. \quad (49)$$

Because of increased transparency at lower temperature, $T_e \lesssim 2000$ K is unlikely. Because of the observed weakness of hydrogen lines in SN I spectra, it might be more reasonable to consider a hydrogen-poor envelope. For a composition of mostly ${}^4\text{He}$, $T_e \gtrsim 6000$ K seems plausible. A systematic study of extended envelopes with nonsolar compositions would be helpful. At present we can only conclude that small radii ($R \lesssim 10^{13}$ cm) seem more likely than large, but no proof of the nonexistence of larger initial radii has been devised.

There are several observations which bear on this question. Kirshner, Arp, and Dunlap (1976) found for 1975a in NGC 2207 that at 5 days before maximum light the photospheric temperature was near 12,000 K, which seems to agree better with a purely radioactive model (see eq. [41], Table 1, and below). The OAO 2 observations of 1972e (Holm, Wu, and Caldwell 1974) show an ultraviolet deficit, but these data were obtained past maximum light, and are therefore not conclusive for this question. The Asiago composite light curve (Barbon, Ciatti, and Rosino 1973) shows some considerable scatter at early times; however, this may be due to other causes. It will be interesting to see if any observations exhibit the effects of large initial radius in any Type I supernova.

IV. TRANSPARENCY AND COBALT DECAY

a) More General Source Terms

Nickel-56 decays to ${}^{56}\text{Co}$ by electron capture with a 6.10 day half-life, releasing 2.135 MeV. The ${}^{56}\text{Co}$ then decays to ${}^{56}\text{Fe}$ by electron capture (81%) and positron emission (19%) with a 78.8 day half-life, releasing 4.5675 MeV. After about two mean lives of ${}^{56}\text{Ni}$ (i.e., $2\tau_{\text{Ni}} = 17.6$ days, or $xy \approx 1$) the energy release from ${}^{56}\text{Co}$ decay exceeds that from ${}^{56}\text{Ni}$. This occurs near the time of maximum light. Therefore, the description of later parts of the light curve must be generalized to include the effect of ${}^{56}\text{Co}$ decay.

The analysis which led to (31) and (48) above demanded *no significant restriction on the functional form of the time-dependence of the radioactive energy source*. This method may be used for far more complex time-behavior than the simple exponential decay given in (9).

A direct generalization of (9) to include ^{56}Co decay would not be correct either, because this energy is released as γ -rays (and positrons) which may escape from the expanding matter (see Arnett 1979; Colgate, Petschek, and Kriese 1980). A detailed quantitative discussion of this effect is beyond the scope of this paper. The numerical results of Colgate, Petschek, and Kriese (1980) suggest that such a generalization will be successful; this could provide a self-consistent model for the entire Type I light curve. Note that considerable progress on understanding the very late behavior has been made (Meyerott 1978, 1980; Axelrod 1980) within the framework of this same physical model.

As an exploratory procedure we will use the "deposition function," D , of Colgate, Petschek, and Kriese (1980). They find

$$D = G[1 + 2G(1 - G)(1 - 0.75G)], \quad (50)$$

where

$$G \equiv \tau / (\tau + 1.6) \quad (51)$$

and τ is the "optical" depth for γ -rays or for positrons. Here D is defined as the fraction of decay energy which is available to heat the matter. Using their estimates of the average cross sections, we have

$$\tau_\gamma \approx 55.3(0.1/\kappa)y^2 / [v_{sc}(0.1 + 2xy)^2]; \quad (52)$$

and for positrons,

$$\tau_+ \approx 355\tau_\gamma. \quad (53)$$

Applying these deposition functions D as factors to the γ -ray energy release from ^{56}Ni and ^{56}Co , and to the positron kinetic energy release from ^{56}Co , gives us a generalized source term to replace the simple exponential decay of ^{56}Ni given in (9).

b) Model Parameters

There are many choices of total mass (M), mass of ^{56}Ni (M_{Ni}), and velocity scale (v_{sc}) which should be examined. To illustrate the method, we will use the choices shown in Table 2. Initial radii are assumed to be small: $R(0) \ll 10^{13}$ cm. The first three models may be taken to represent the result of degenerate ignition of ^{12}C in a core near the Chandrasekhar limiting mass. It is assumed that different amounts of ^{56}Ni are synthesized. The transformation $2\ ^{12}\text{C} + 2\ ^{16}\text{O} \rightarrow ^{56}\text{Ni}$ releases 44.4 MeV or $q = 0.76 \times 10^{18}$ ergs per gram of fuel burned. This energy is transformed into kinetic energy of expansion so that M_{Ni} and v_s are related. For uniform density,

$$v_{sc}^2 = 3/5(2E_{\text{SN}}/M). \quad (54)$$

Hydrodynamic models tend to give a structure with density increasing inward; this results from shock steepening in an initial density gradient, and from the initial gradient itself. The faster moving matter becomes transparent faster, so that if we take v_{sc} from the photospheric fluid velocity near maximum light, this value is not far from the uniform-density estimate. For this reason, and for consistency with Colgate, Petschek, and Kriese (1980), a uniform-density structure will be used. Now we also have $E_{\text{SN}} = M_{\text{Ni}}q$, so

$$(v_{sc}/10^9 \text{ cm s}^{-1})^2 \approx 2.53(M_{\text{Ni}}/M). \quad (55)$$

The last two models may be taken to represent the results of core collapse of an evolved helium star of total mass about $2.7 M_\odot$. The formation of the neutron star gives 10^{51} ergs of kinetic energy; the shock, some ^{56}Ni .

These choices are not intended to survey all the possibilities, but merely to examine two classes of models which have been widely discussed. Detailed characteristics of models A and C are tabulated in the appendix; they represent the range of behavior of all five models.

c) Bolometric Luminosity

The bright Type I supernova 1972e was observed shortly after peak, and for about 700 days thereafter. In

TABLE 2
MODEL PARAMETERS

Model	Mass/ M_\odot	M_{Ni}/M_\odot	$v_{sc}/10^9 \text{ cm s}^{-1}$	Cause
A	1.45	0.5	0.94	thermonuclear
B	1.45	0.7	1.11	thermonuclear
C	1.45	1.0	1.32	thermonuclear
D	1.24	0.4	1.16	collapse
E	1.24	0.8	1.16	collapse

the postpeak epoch, most of the energy radiated was in the B and V bands (Kirshner *et al.* 1973; Holm, Wu, and Caldwell 1974; Ardeburg and de Groot 1973). It is interesting, therefore, to compare the shape of the bolometric luminosity curve with that observed in the V and B bands.

Before proceeding, we note a considerable simplification: the dimensionless luminosity Λ is virtually identical for models C, D, and E because they have essentially the same value for the parameter γ (see [42]). The actual luminosity differs because it scales with M_{Ni} (see [36]). For models C and E the effective temperatures are also very similar because $M_{\text{Ni}}/v_{\text{sc}}^2$ is similar. This is an indication of a general result: *on the basis of the physics described by these solutions, it is impossible to distinguish between thermonuclear and collapse models.* Such a choice must be based on the explosion models themselves (can they provide the necessary values of M , M_{Ni} , and v_{sc} in a self-consistent way?), or on the nonexistence of a compact object (neutron star or black hole) in the observed remnant.

In Figure 3a the dimensionless luminosity Λ is compared with observed B and V magnitudes for the Type I supernova 1970j in NGC 7619. Model A lies along the B points in the early part of the peak when they carry most of the energy, and along the V points when they dominate. Model C falls too quickly after peak light. However, in Figure 3b, which has data from the bright Type I supernova 1972e in NGC 5253, the situation is reversed. Model A falls too slowly while model C has the correct slope.

The steepness of the decline in Λ is determined by the parameter γ , which for the thermonuclear models de-

pends upon M_{Ni} , the amount of ^{56}Ni synthesized. For the collapse models γ may vary with both the strength of the explosion and the amount of ^{56}Ni ejected. The difference in 1970j and 1972e corresponds (in both cases) to a factor of 2 variation in explosion energy. The behavior seems to be related to the "fast" and "slow" subclasses of Type I supernovae defined by Barbon, Ciatti, and Rosino (1973). Although their discussion concerned the B magnitudes, the same behavior is apparent here also. Roughly speaking, a bigger explosion gives a bigger peak, but also faster expansion and hence quicker decline due to transparency.

d) The Blackbody Supernova

In an attempt to obtain a more detailed understanding of Type I supernovae, we introduce the hypothetical construct of a "blackbody supernova." In this construct the radiation escaping has a blackbody spectrum corresponding to the temperature of the photosphere. The difficulty then lies in deciding where the photosphere is.

Not only does the expanding supernova become transparent to γ -rays, but also to thermal photons. This occurs only slightly later than γ -transparency because the Thomson cross section for electron scattering is only slightly larger than the Klein-Nishina cross section at the appropriate γ -ray energies. This transparency to thermal photons has two effects of fundamental importance: (1) it keeps the effective temperature of the photosphere hotter, and (2) it causes much of the radiation to be "nebular" rather than "photospheric." This epoch of the SN I evolution provides a fascinating problem in radiative transfer. Unfortunately it is also a

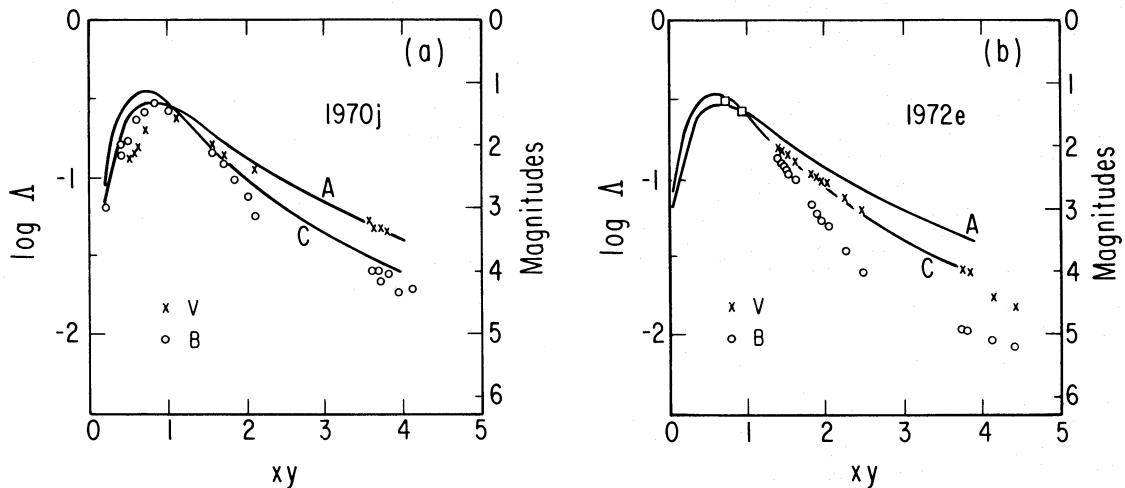


FIG. 3.—Evolution of bolometric luminosity for models A and C (see text) compared with observed B and V magnitudes. (a) SN I 1970j. Model C falls more swiftly than the observed V magnitudes (*crosses*), while model A seems to have the same shape as the total B and V luminosity. (b) SN I 1972e. Here model A falls too slowly, but model C seems to better represent the total B and V luminosity. Both vertical and horizontal zero points (distance and explosion time) were adjusted so the observations and theoretical curves coincided. It is the shape of the curves that is significant in this comparison.

formidable one, and quite beyond the scope of this paper.

We will use simple approximations to explore the onset of transparency. First we will determine an effective temperature from

$$\sigma T_e^4 = L/4\pi R_e^2, \tag{56}$$

where $R_e = R - 2/3\lambda$, and λ is the transport mean free path for thermal photons. This is the Eddington solution to the Milne problem, and appropriate to planar geometry. This rapidly becomes inaccurate as $\lambda \rightarrow R$, due to a number of effects (spherical geometry, absorption versus scattering, energy source outside the photosphere, variable opacity, "nebular" line emission, Doppler effects, etc.). Although imperfect, this approximation does allow us to follow the evolution of the Type I supernova well past maximum light before it breaks down disastrously.

Following Kirshner *et al.* (1973) we introduce *AB* magnitudes defined by

$$AB_\nu = -2.5 \log f_\nu - 48.60 \tag{57}$$

where f_ν is the flux density in units of $\text{ergs s}^{-1} \text{cm}^{-2} \text{Hz}^{-1}$. Their *AB*(5500) is the flux density obtained from scans near 5500 Å, and corresponds closely with the *V* magnitude. For a blackbody,

$$f_\nu = \frac{T_e^4}{\nu} \left(\frac{15}{\pi^4} \frac{x^4}{e^x - 1} \right), \tag{58}$$

where $x = h\nu/kT$. We identify *U* with 3590 Å and *B* with 4400 Å for our blackbody. We define a distance-independent quantity for the *U* band,

$$\phi(3590) = AB(3590) - 5 \log D(\text{Mpc}) - 1.086\chi D, \tag{59}$$

and similarly for *B* and *V*. Here χ is the extinction and *D* the distance to the source. Then

$$\phi(3590) = C_U - 2.5 \log \Lambda - 2.5 \log \left[\frac{x_U^4}{\exp(x_U) - 1} \right]; \tag{60}$$

and similarly for *B* and *V*. The constants C_i and $T_4 X_i$ are given in Table 3; T_4 denotes $T/10^4$ K, and $i = U, B,$ and *V*.

These $\phi_U, \phi_B,$ and ϕ_V represent *U, B,* and *V* magnitudes of our "blackbody supernova" at $D = 1$ Mpc if we add the corrections Δ_i for the zero scale of the *UBV* system ($U \approx \phi_U - 1.22$ and so on). The corrections were obtained from the absolute flux calibration given by Johnson (1966). The ϕ magnitudes are useful for several

TABLE 3
UBV COEFFICIENTS

<i>i</i>	C_i	$T_4 X_i$	Δ_i
<i>U</i> ...	6.000	4.008	-1.22
<i>B</i> ...	5.761	3.252	+0.22
<i>V</i> ...	5.519	2.616	+0.05

reasons. They are functionally similar to *UBV* magnitudes (the shapes of theoretical and observational graphs can be compared easily), and they represent an absolute scale. The ϕ 's are roughly equal for temperatures near 10^4 K. At $T_4 = 1.31$, $\phi_U - \phi_B = 0$ and $\phi_B - \phi_V = -0.11$; while at $T_4 = 1.05$, $\phi_U - \phi_B \approx 0.14$ and $\phi_B - \phi_V \approx 0$. The scales of the *UBV* system were chosen so that for a *real* spectrum (an A0 dwarf), $U = B = V$. Because real stars have an ultraviolet deficiency relative to a blackbody, the correction Δ_U is particularly significant. However, *real* supernovae also have a large deficiency so that these corrections tend to cancel when we compare observed *UBV* with the ϕ magnitudes of our blackbody supernova.

The behavior of the ϕ magnitudes for a blackbody supernova (model C) is shown in Figure 4. Before maximum light the shapes of all three of the curves are similar. The peak occurs first in ϕ_U , then ϕ_B , then ϕ_V ; the interval is $\Delta_{xy} \approx 0.1$ or about 2 days. This is in excellent agreement with the estimates of Ardeberg and de Groot (1973) for 1972e and the results of Bertola (1964) for the peculiar Type I supernova in NGC 1073 discovered in 1962. The decline from peak becomes linear on the magnitude scale (exponential in flux), with a *different* slope for each band. In our previous discussion of the bolometric curve (Λ) and the *V* light curve of 1972e we identified the time JD 2441455 with $xy = 1.4$. This synchronized the time scales. Table 4 gives the

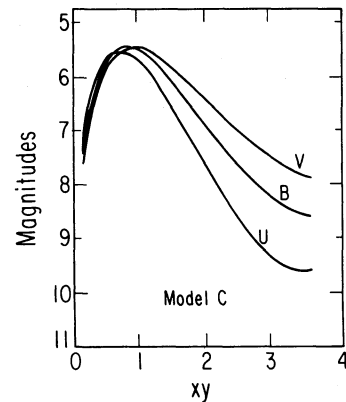


FIG. 4.—*UBV* magnitudes versus time (*xy*) for model C. The curves have maxima of different times and different slopes after maximum light even though the same energy source powers all three. This is an effect of decreasing photospheric temperature.

TABLE 4
SLOPES OF LIGHT CURVES (in magnitudes per day)
FOR 1972e AT JD 2,441,455 AND MODEL C

Slope	1972e	Model C
dV/dt	0.053	0.060
dB/dt	0.080	0.088
dU/dt	0.114	0.114

observed slopes of the UBV light curves and the ϕ magnitudes at this time. The agreement may be misleadingly good; the effective temperature of the model is $T_e \approx 7800$ K while Kirshner *et al.* (1973) found $T_e \approx 10,000$ K. Their temperature was chosen to fit the *shape* of the visual spectrum; it is simply not clear whether or not our effective temperature would imply a similar *shape* when processed through a realistic atmosphere.

In Figure 5 the ϕ_B and ϕ_V magnitudes from model A are compared with the B and V magnitudes of Barbon, Ciatti, and Rosino (1973) for 1970j in NGC 7619. Three adjustable parameters were picked: the time axis and the assumed distance were shifted until the B curve fitted the ϕ_B curve. The V curve was then shifted upward (slightly) to the data. The observational errors are estimated to be about ± 0.15 mag. The agreement is excellent until time $xy \approx 2.2$; then V is brighter and B dimmer than the model. At this time the photosphere is at 88% of the radius, so about one-third of the volume is "transparent." Our neglect of "nebular" effects begins to be serious, so a discrepancy is to be expected. Prior to this time the blackbody model represents the observed B and V magnitudes quite well; for later times the V curve follows the bolometric luminosity as noted before (see Fig. 3a).

e) Near Maximum Light

Kirshner, Arp, and Dunlap (1976) observed Type I supernova 1975a in NGC 2207, beginning about 7 days before maximum light and continuing until shortly after maximum. At 5 days before maximum they found a radius of 1.0×10^{15} cm, at temperature of 12,000 K and

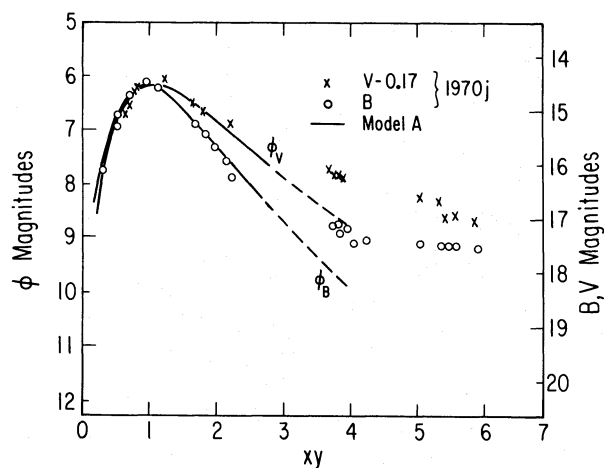


FIG. 5.—Magnitudes ϕ_B and ϕ_V for model A compared to SN I 1970j. Time synchronization and distance were fixed by overlaying the theoretical ϕ_B curve with the observed B curve (open circles). The V curve was shifted by -0.17 mag for comparison with ϕ_V . The agreement is good until $xy > 2$, at which time nebular effects become important.

a fluid velocity of $11,600$ km s^{-1} . The radius estimate depends on the distance attributed to NGC 2207. Table 5 gives the corresponding quantities for the models, all taken at $xy = 0.6$ which is about 5 days before maximum light. Within the uncertainties imposed by our ignorance of supernova atmospheres, the agreement is good for all five models. There is a weak indication that 1975a was neither "fast" nor "slow," but intermediate between 1972e and 1970, because model B fits the velocity better than A or C; however, model E (as "fast" as model C) also fits the velocity.

Far more important is the variation in the ϕ_B magnitude shown. For models A and C the difference of 0.89 mag corresponds roughly to the fact that model C had twice as much ^{56}Ni . If actual Type I supernovae are like these models, then they are *not* an especially uniform set of standard candles. Branch and Bettis (1978) estimate the standard deviation in intrinsic luminosity of Type I supernovae to be $\sigma < 0.5$ mag, corresponding to a range

TABLE 5
COMPARISON OF THEORY WITH OBSERVATIONS OF 1975a

Model	$v_e/10^4$ km s^{-1}	$R_e/10^{15}$ cm	$T_e/10^4$ K	ϕ_B
A	0.93	0.85	1.25	6.55
B	1.10	1.00	1.29	6.11
C	1.30	1.18	1.32	5.66
D	1.14	1.04	1.12	6.44
E	1.14	1.04	1.34	5.90
SN I 1975a ^a ...	1.16	1.0 ± 0.2	1.2 ± 0.2	

^aKirshner, Arp, and Dunlap 1976.

of variation of about $2\sigma \lesssim 1$ mag. This is slightly above the 0.89 mag difference in models A and C. For these thermonuclear models, (1) the shape of the light curve and (2) the velocity scale may be used to infer the intrinsic luminosity more accurately. The problem of distance determination from supernovae is itself complex, and must be discussed separately.

f) Homogeneity of Spectral Evolution

It has long been known that Type I supernovae form a very homogeneous group with regard to the nature and evolution of their spectra (Minkowski 1964), so much so that the estimated error on the date of maximum light for 1972e was only ± 2 days (Ardeberg and de Groot 1973). How does this striking regularity come about? Stellar spectra are determined primarily by temperature and composition of the photosphere, and to a lesser extent the photospheric density (gravity). To obtain regularity in spectra we must assume regularity in composition (it would be of considerable interest to know how much variation in abundance is allowed by the observations). The requirement that the luminosity peak not be too broad and that the velocity scale be of order 10^9 cm s⁻¹ constrains the already weak dependence on photospheric density.

The remaining condition is that the temperature scale be consistent from supernova to supernova. Despite complications from shock effects (§ III) and transparency (discussed above), this condition is essentially reduced to a consideration of equation (41), or, more generally,

$$T_e \propto (M_{\text{Ni}}^0/v_{\text{sc}}^2)^{1/4} (\Lambda/x^2y^2)^{1/4}. \quad (61)$$

The *shape* of the luminosity curve fixes the factor Λ/x^2y^2 . Thus, to keep the temperature scale consistent, we would require

$$M_{\text{Ni}}^0 \propto v_{\text{sc}}^2. \quad (62)$$

This is just equation (55), a *necessary* condition for the degenerate thermonuclear explosion. It is a *possible* condition for a gravitational collapse supernova (a more violent explosion might process and eject more ⁵⁶Ni), but is not a necessary one. Further, the constant of proportionality in (62) is also given correctly by (55); i.e., for $2\ ^{12}\text{C} + 2\ ^{16}\text{O} \rightarrow\ ^{56}\text{Ni}$ (see § IVe). Figure 6 shows the evolution of effective temperature T_e for models A, B, and C. While the precise shape of these curves may be modified by more sophisticated treatment of the atmosphere/nebula, their similarity to one another will probably not be affected.

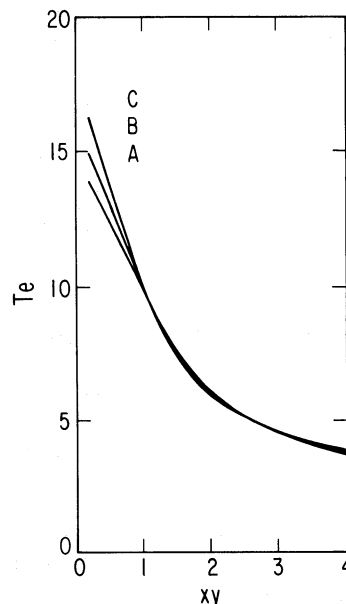


FIG. 6.—Effective temperature versus time for the “degenerate ignition” models A, B, and C. This strong similarity in effective temperature at any given epoch, despite a considerable difference in explosion strength, may contribute to the observed uniformity of spectral evolution of Type I supernovae.

V. CONCLUSION

a) Connections to Other Recent Work

This analytic work developed as a consequence of numerical calculations by the author of the explosion of low mass ($M_{\alpha} \approx 3M_{\odot}$) helium cores, and the realization that the problem was analytically tractable (Arnett 1979). Schurmann (1982) has numerically examined the light curves and spectra from homologously expanding models with steep density gradients; his results are in essential agreement with those presented here. Chevalier (1981) has numerically constructed simple hydrodynamic models of the explosion of an accreting white dwarf star, and used the “blackbody supernova” approximation to compare with observations. His results are in agreement with the analytic models presented above (see model C). The review of presupernova models by Sugimoto and Nomoto (1980) discusses possible progenitors for such events; see also Woosley, Weaver, and Taam (1980).

The X-ray spectrum of Tycho’s remnant (a Type I supernova) has been obtained by *Einstein* Observatory. The argument (Becker *et al.* 1980) that the abundances derived from the X-ray features are evidence against Type I light curves being powered by ⁵⁶Ni and ⁵⁶Co decay has several flaws: the abundance determinations (1) assume ionization equilibrium, (2) assume homogeneous composition, and (3) are inconsistent in that the

abundances determined are not the same as the abundances used to model the spectra. It is likely that Tycho's supernova did synthesize a lot of iron (0.5–1 M_{\odot}). It is not clear in what form such iron would be (gas, solid drops, dust?) or whether it would be in the matter currently heated by the shock formed from interaction with slower material. It is therefore of considerable importance to understand precisely why Becker *et al.* (1980) did not discover a strong iron line in Tycho's X-ray spectrum.

The work of Meyerott (1978, 1980) and Axelrod (1980) on the optical spectra at late times ($t \gtrsim 70$ days or $xy \gtrsim 4$) strongly supports the decay of ^{56}Co as the cause of the exponential tail in luminosity. Branch (1980) finds no indication of cobalt lines in the spectrum of 1972e at velocities $\gtrsim 8,000 \text{ km s}^{-1}$ (Axelrod obtains a similar constraint from the late spectra). This and the Becker *et al.* (1980) result rule out models which convert essentially all the star to ^{56}Ni . However, this is not awkward if the explosion burns to completion only the inner part of the star. This important clue cannot yet be further understood because our knowledge of the nature of the hydrodynamics associated with the thermonuclear burning is inadequate.

b) Further Developments

We now have analytic solutions which describe the main features of Type I supernovae. Two large areas of ignorance remain: (1) How are the optical spectra formed (the atmosphere/nebula problem)? (2) What evolutionary paths lead to this result? There are several good prospects for immediate progress. An extensive comparison of these models with observations will define the allowed range of parameters such as total mass, nickel mass and explosion energy. These models can be generalized to include nonuniform density distributions and more realistic treatment of γ -ray and thermal photon escape. It should be possible to construct a better, independent distance scale from Type I supernovae.

The author would like to thank T. Axelrod, D. Branch, R. Chevalier, S. A. Colgate, R. I. Epstein, R. Meyerott, K. Nomoto, S. Schurmann, T. Weaver, and S. E. Woosley for sending preprints of their recent work. The calculations reported here were done on an Apple II Plus computer. This work was begun at the Aspen Center for Physics, and was supported in part by NSF grant 78-20392.

APPENDIX

Some important quantitative characteristics of two representative models (A and C, see § IV for details) are presented in Tables 6 and 7. The notation is the same as in the text. The quantity xy is time since explosion in units of 17.6 days, Λ is the bolometric luminosity in ^{56}Ni units (see eq. [36]), τ_{γ} is the total (average) "optical" depth for γ -rays (see eq. [52]), v_e is the fluid velocity at the photosphere in units of $10,000 \text{ km s}^{-1}$, R_e is the photospheric radius in units of 10^{15} cm (see eq. [56]), T_e is the effective temperature in units of 10^4 K , L_{43} is the bolometric luminosity in units of $10^{43} \text{ ergs s}^{-1}$, and ϕ_U , ϕ_B , and ϕ_V are the magnitudes of a "blackbody supernova" at 1 Mpc as defined in § IVd (especially eqs. [57]–[60] and Table 3).

TABLE 6
MODEL A

xy	Λ	τ_{γ}	v_e	R_e	T_e	L_{43}	ϕ_U	ϕ_B	ϕ_V
0.2 ...	0.0598	153.5	0.934	0.284	1.49	0.285	8.36	8.42	8.58
0.4 ...	0.174	47.4	0.931	0.567	1.38	0.824	7.11	7.14	7.27
0.6 ...	0.265	22.7	0.927	0.846	1.25	1.26	6.57	6.55	6.64
0.8 ...	0.301	13.3	0.920	1.120	1.12	1.43	6.37	6.28	6.32
1.....	0.289	8.70	0.912	1.39	1.00	1.37	6.40	6.23	6.20
1.2 ...	0.253	6.14	0.902	1.65	0.888	1.20	6.59	6.32	6.21
1.4 ...	0.211	4.56	0.890	1.90	0.791	1.00	6.89	6.51	6.31
1.6 ...	0.176	3.52	0.876	2.13	0.712	0.834	7.24	6.75	6.46
1.8 ...	0.148	2.81	0.861	2.36	0.650	0.702	7.62	7.02	6.65
2.....	0.127	2.28	0.843	2.56	0.598	0.601	8.01	7.30	6.84
2.4 ...	0.0967	1.60	0.803	2.93	0.523	0.499	8.76	7.86	7.24
2.8 ...	0.0760	1.18	0.755	3.22	0.470	0.361	9.50	8.42	7.65
3.2 ...	0.060	0.908	0.700	3.41	0.431	0.287	10.20	8.97	8.07
3.6 ...	0.0485	0.72	0.638	3.49	0.403	0.231	10.85	9.49	8.47
4.....	0.0393	0.585	0.569	3.46	0.385	0.187	11.40	9.93	8.84

TABLE 7
MODEL C

xy	Λ	τ_γ	v_e	R_e	T_e	L_{43}	ϕ_U	ϕ_B	ϕ_V
0.2 ...	0.0829	77.0	1.317	0.401	1.62	0.787	7.36	7.46	7.65
0.4 ...	0.228	23.8	1.31	0.797	1.48	2.17	6.14	6.20	6.37
0.6 ...	0.320	11.4	1.30	1.183	1.32	3.04	5.66	5.66	5.78
0.8 ...	0.329	6.66	1.28	1.56	1.16	3.13	5.54	5.47	5.52
1.	0.286	4.37	1.255	1.91	1.01	2.27	5.66	5.49	5.47
1.2 ...	0.229	3.08	1.227	2.24	0.884	2.18	5.94	5.67	5.56
1.4 ...	0.180	2.29	1.19	2.54	0.781	1.71	6.32	5.93	5.73
1.6 ...	0.143	1.77	1.16	2.81	0.700	1.36	6.75	6.24	5.94
1.8 ...	0.115	1.41	1.11	3.04	0.638	1.10	7.18	6.56	6.17
2.	0.0950	1.14	1.06	3.23	0.590	0.902	7.61	6.88	6.41
2.4 ...	0.0672	0.802	0.949	3.46	0.522	0.638	8.41	7.50	6.88
2.8 ...	0.0496	0.593	0.815	3.47	0.484	0.471	9.07	8.04	7.32
3.2 ...	0.0377	0.456	0.660	3.21	0.470	0.359	9.51	8.43	7.66
3.6 ...	0.0296	0.361	0.485	2.65	0.486	0.281	9.61	8.59	7.87

REFERENCES

- Ardeburg, A., and de Groot, M. 1973, *Astr. Ap.*, **28**, 295.
 Arnett, W. D. 1979, *Ap. J. (Letters)*, **230**, L37.
 ———. 1980, *Ap. J.*, **237**, 541 (A80).
 Axelrod, T. 1980, Ph.D. thesis, University of California at Santa Cruz, UCRL-52994.
 Barbon, R., Ciatti, F., and Rosino, L. 1973, *Astr. Ap.*, **25**, 24.
 Becker, R. H., Holt, S., Smith, B. W., White, N. E., Boldt, E. A., Mushotsky, R. F., and Serlemitsos, P. J. 1980, *Ap. J. (Letters)*, **235**, L5.
 Bertola, F. 1964, *Ann. d'Ap.*, **27**, 319.
 Branch, D. 1980, preprint.
 Branch, D., and Bettis, C. 1978, *A. J.*, **83**, 224.
 Chevalier, R. A. 1981, *Ap. J.*, **246**, 267.
 Chevalier, R. A., and Klein, R. I. 1979, *Ap. J.*, **234**, 597.
 Colgate, S. A., and McKee, C. 1969, *Ap. J.*, **157**, 623.
 Colgate, S. A., Petschek, A. G., and Kriese, J. T. 1980, *Ap. J. (Letters)*, **237**, L81.
 Epstein, R. I. 1980, preprint.
 Falk, S. W. 1978, *Ap. J. (Letters)*, **225**, L133.
 Holm, A. V., Wu, C.-C., and Caldwell, J. J. 1974, *Pub. A.S.P.*, **86**, 296.
 Johnson, H. L. 1966, *Ann. Rev. Astr. Ap.*, **4**, 193.
 Karp, A. H., Chan, K. L., Lasher, G. J., and Salpeter, E. E. 1977, *Ap. J.*, **214**, 161.
 Kirshner, R. P., Arp, H. C., and Dunlap, J. R. 1976, *Ap. J.*, **207**, 44.
 Kirshner, R. P., Willner, S. P., Becklin, E. E., Neugebauer, G., and Oke, J. B. 1973, *Ap. J. (Letters)*, **180**, L97.
 Lasher, G. 1975, *Ap. J.*, **201**, 194.
 Lasher, G., and Chan, K. L. 1979, *Ap. J.*, **230**, 742.
 Meyerott, R. E. 1978, *Ap. J.*, **221**, 975.
 ———. 1980, *Ap. J.*, **239**, 257.
 Minkowski, R. 1964, *Ann. Rev. Astr. Ap.*, **2**, 247.
 Schurmann, S. R. 1982, in preparation.
 Sugimoto, D., and Nomoto, K. 1980, *Space Sci. Rev.*, **25**, 155.
 Woosley, S. E., Weaver, T. A., and Taam, R. E. 1980, "Models for Type I Supernovae", in Workshop on Atomic Physics and Spectroscopy for Supernova Spectra, La Jolla Institute, to be published.

W. DAVID ARNETT: Astronomy and Astrophysics Center, University of Chicago, 5640 S. Ellis Avenue, Chicago IL 60637